Experimental Characterization of Colorless Phase Retrieval Under Ultrafast Wavelength Drift for Upstream PON Transmission

Hanzi Huang[1,2], Haoshuo Chen[2], Nicolas K. Fontaine[2], Yingxiong Song[1], Mikael Mazur[2], Lauren Dallachiesa[2], Yuanhang Zhang[2], Chenhui Ye[3], Dora Van Veen[2], Vincent Houtsma[2], Roland Ryf[2] and David T. Neilson[2]

[1] Key Laboratory of Specialty Fiber Optics and Optical Access Networks, Joint International Research Laboratory of Specialty Fiber Optics and Advanced Communication, Shanghai Institute for Advanced Communication and Data Science, Shanghai University, 200444 Shanghai, China
[2] Nokia Bell Labs, 600 Mountain Ave, Murray Hill, NJ 07974, USA
[3] Nokia Bell Labs, Shanghai, 201206, China

haoshuo.chen@nokia-bell-labs.com

Abstract: We successfully recover 40-GBaud QPSK signal under ultrafast wavelength drift up to 20,000 nm/s after 40-km single-mode fiber (SMF) transmission employing colorless phase retrieval receiver tackling upstream burst-mode issues in high-speed PON. © 2022 The Author(s)

1. Introduction

To support the fast growing bandwidth demands by emerging applications such as fixed-mobile convergence for 5G, ultra high definition video streaming, the Internet of Things and remote working/business/education, passive optical networks (PONs) with higher speed as cost-effective transport solutions are being pursued. Among the potential access solutions, coherent technology based PON systems attract researchers' attentions due to its higher receiver sensitivity, enabling digital chromatic dispersion compensation and adaptive advanced modulation formats to enhance the network capacity as well as coverage [1, 2]. However, since coherent reception technology is based on detecting the beating electric fields between the signal and local oscillator (LO) [3], precise wavelength alignment of each transmitting optical network unit (ONU) with LO is needed to ensure that the down-converted intermediate frequency (IF) signal lies within the receiver electrical bandwidth (see Fig. 1(a)). Moreover, wavelength drift happens when on-off switching a regular distributed feedback (DFB) laser for ONU transmitters in generating a bust-mode (BM) signal for upstream, as shown in Fig. 1(b), and avoiding it needs extra optical shutters such as acoustic optical modulators (AOMs) or semiconductor optical amplifiers (SOAs), which greatly raise the cost. As a result, the constraints on wavelength accuracy as well as stability raise challenges associated with upstream BM reception for coherent PON, which force network designers to introduce precise wavelength management and control mechanisms for each ONU, and hinder the coherent technology to be the plug-and-play upgrade solution for the prevailing time-division multiplexing (TDM) PON architectures. On the other hand, phase retrieval (PR) receiver (Rx) can perform similarly as conventional coherent Rx with the capabilities in full field signal reconstruction and digital dispersion compensation but without the need of LO [4]. The PR Rx retrieves signal phases by comparing intensity measurements therefore can avoid the requirement to align ONU center wavelengths and is tolerant to frequency drifts, both of which are essential for upstream PON transmission [5].

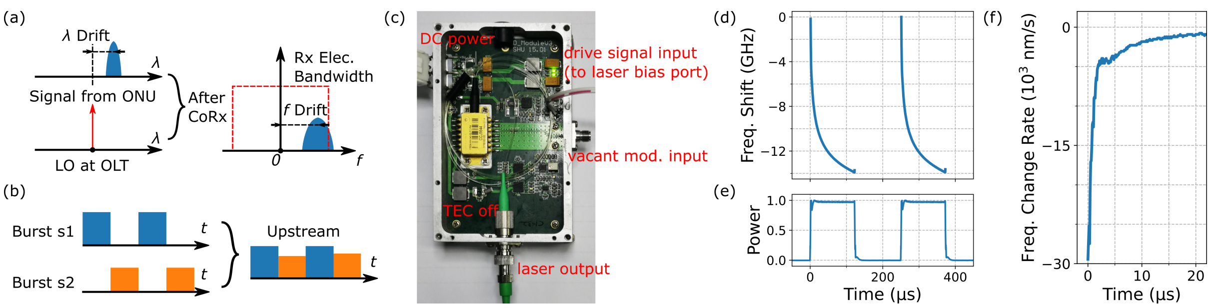

Fig. 1: (a) Schematic drawing of coherent reception under a wavelength misalignment in PON systems, (b) schematic of upstream BM transmission, (c) the photograph of the measured DFB laser, (d) measured frequency shift and (e) intensity of the DFB laser operating in BM mode, (f) measured instantaneous frequency change rate at a burst start. (TEC: thermoelectric cooler)

In this paper, we characterize the performance of the colorless PR Rx under ultrafast wavelength drift for BM 40-GBaud QPSK signal reception. We experimentally demonstrate full C-band (from 1525 to 1565 nm) full-filed reconstruction within a single sweep of a swept-wavelength laser (SWL) under wavelength drift up to 20,000 nm/s. The robustness of PR Rx to fast wavelength drift enables directly switching on-off the regular uncooled DFB lasers at ONUs to generate BM upstream signals. By equipping optical line terminal (OLT) with the PR Rx, the requirements for digital dispersion compensation, complex modulation formats and wavelength independent reception in upstream can be met, allowing smooth evolution towards >100G PONs.

2. DFB Lasers Under Upstream BM Operation

Under BM operation, DFB lasers experience spectral broadening and drift due to a combination of transient, adiabatic and thermal chirp [6], which can be up to 157 GHz [7]. The frequency excursion measured by heterodyne beating of a conventional 40-mW DFB laser in Fig. 1(c) under a 4-kHz 50% duty cycle time-gated drive signal is shown in Fig. 1(d). The DFB laser is constantly switched between non-lighting and emitting, whose intensity is captured by a photodiode and plotted in Fig. 1(e). Heterodyne detection is applied to measure its frequency drift which is most pronounced at the start of the burst (from OFF to ON state) and reaches its maximum up to ∼16 GHz at the end of the burst. Figure 1(f) shows the measured frequency change rate by calculating the differential of frequency-time curve. The instantaneous frequency change rate can be up to 30,000 nm/s at the start of the burst and decreases over time. This fast and broadband frequency excursion not only requires extra Rx electrical bandwidth and algorithm complexity in conventional coherent detection but also degrades system performance due to the existence of a large frequency offset, especially for high order modulation formats.

3. Phase Retrieval Field Recovery Under Frequency Drift

Compared with coherent Rx, PR Rx can be regarded as a colorless full field recovery scheme using complementary intensity measurements over mixed complex symbols to recover the phases of modulated signal [8]. Figure 2(a) gives a schematics of a PR Rx with space-time diversity, which has a Rx sensitivity close to coherent reception [4]. $\vec{\mathbf{P}}$, $\boldsymbol{T}$, $\boldsymbol{H}$ and $\mathbf{f}_D$ denote the transfer function of an optical splitter, array of waveguide delay lines, optical coupler and dispersive element, respectively. I_A and I_B denote the intensity measurements. To obtain a strong symbol mixing effect, the amount of dispersion in $\mathbf{f}_D$ is set to -330 ps/nm and temporal delays in $\boldsymbol{T}$ are optimized to 0, 10 and 20 T_s, where T_s denotes symbol period. As shown in Fig. 2(b), modified from Gerchberg-Saxton algorithm, PR algorithm uses I_A and I_B to update phases θ_A and θ_B within each iteration.

For the PR Rx, a time-varying carrier frequency gives a phase deviation for mixed symbols and results in intensity deviation at I_A and I_B compared to a stable carrier frequency. The symbol mixing effect in the PR Rx can be quantified by the power of impulse response shown in Fig. 2(c), where a transmission distance of 40 km induces ∼20 symbol mixing for 40-GBaud symbol rate. A total symbol mixing ∼40 symbols can be obtained by considering the temporal delays in $\boldsymbol{T}$. Under a linearly increasing carrier frequency, the adjacent symbols will have a quadratic phase offset distribution, as shown in Fig. 2(d). For a fixed frequency drift rate of 40,000 nm/s, simulated BER performance versus OSNR with different delay increments in the PR Rx is plotted in Fig. 2(e), which shows a shorter symbol mixing length is more resistant to frequency drift. Simulated BER curves versus OSNR under different frequency change rates for BTB and 40-km SMF transmission are shown in Fig. 2(f). Simulated results show that a frequency drift of 40,000 nm/s does not induce significant phase deviation for a 40-GBaud signal (only ∼0.5 degree for the 40th symbol), and the performance of the PR Rx is very robust to frequency drift for both BTB and 40-km transmission cases.

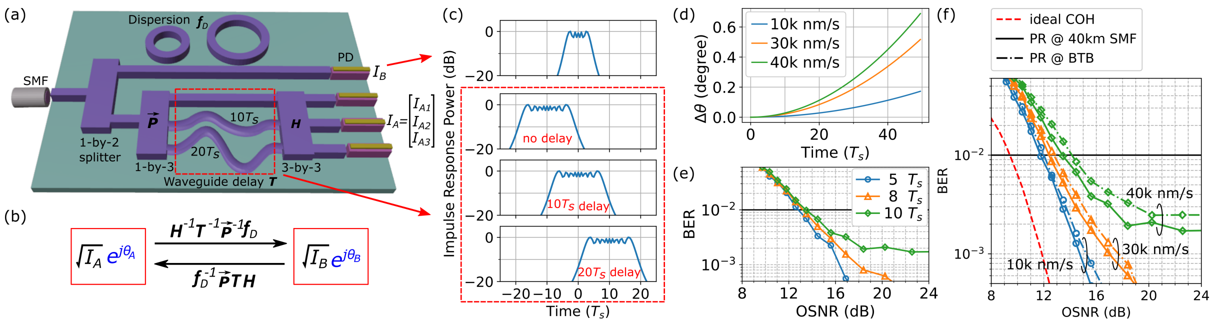

Fig. 2: Schematics of (a) the PR Rx with space-time diversity, (b) iterative PR algorithm, (c) the power of impulse response after 40-km SMF transmission, (d) phase offset $\Delta\theta$ versus time, simulated BERs versus OSNR (e) for different delay increments in PR Rx under a 40,000-nm/s frequency change rate and (f) under different frequency change rates for BTB and 40-km transmission. (T_s: symbol period)

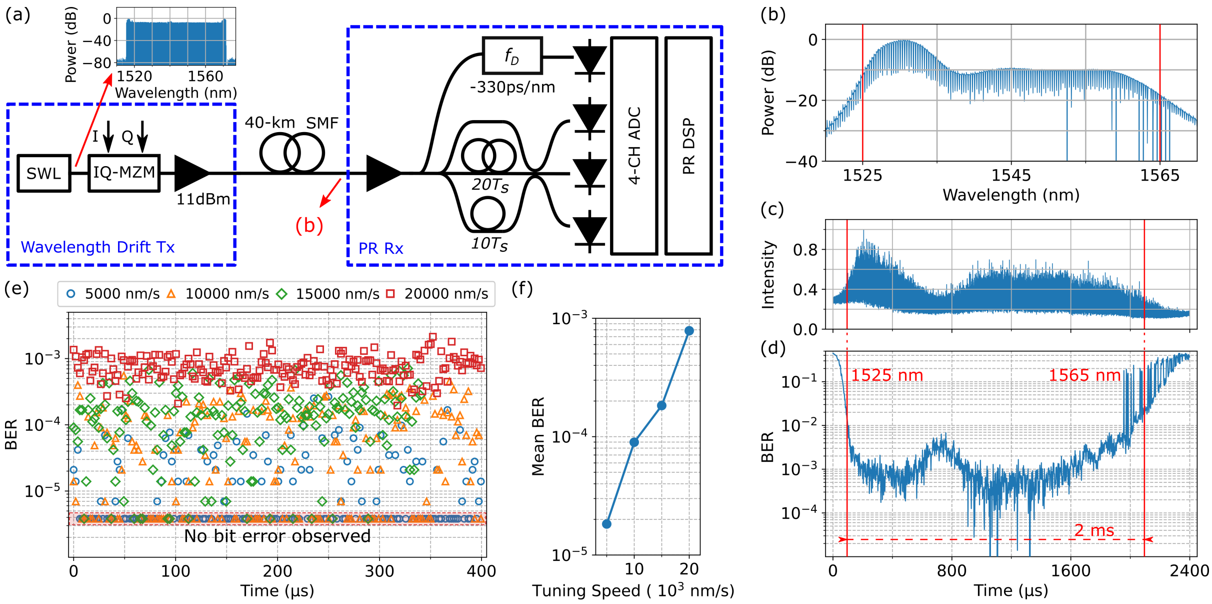

Fig. 3: (a) Experimental setup of colorless direct detection PR with a SWL emulating a wavelength drift light source, (b) measured optical spectrum at the receiver, (c) temporal intensity waveform captured by the ADC, (d) BER over 2400 μs under 20,000-nm/s tuning speed after 40-km SMF, (e) BER and (f) average BER over 400 μs under different wavelength tuning speed for the BTB case.

4. Experimental Setup and Results

Figure 3(a) shows the experimental setup to characterize the PR Rx performance under ultrafast wavelength drift. A SWL is used as the light source for modulation. Nyquist-shaped 40-GBaud QPSK signal with a length of 2^{14} is generated from an in-phase and quadrature Mach-Zehnder (IQ-MZM) modulator driven by a two-channel digital-to-analog converter (DAC). An erbium-doped fiber amplifier (EDFA) is used to boost the output power to 11 dBm. After SMF transmission, the received signal with swept wavelength carrier is amplified and sent into the PR Rx with a total insertion loss around 6 dB. The intensities are detected by four 40-GHz PIN photodiodes and captured at 80 GSa/s using a four-channel analog-to-digital converter (ADC). The captured waveforms are processed offline and a 80-ns preamble is used for synchronization and chromatic dispersion estimation. Signal field reconstruction is done by a parallel block-wise PR algorithm followed by BER calculation with a block length of 8192 symbols. 12.5% pilot symbols are used in PR to facilitate algorithm convergence, resulting in a line rate of 70 Gbps.

The spectrum at the Rx is given in Fig. 3(b) showing an available wavelength span from 1525 to 1565 nm, which is constrained by the EDFA gain profile. The received intensity and measured BER under 20,000-nm/s wavelength tuning speed for 40-km transmission are shown in Fig. 3(c) and (d). The BER curve remain below 1×10^{-2} over the 2-ms time window, and some BER results >1560 nm cannot meet the 1×10^{-2} threshold due to the weak detected intensities with enhanced quantization noises. For BTB transmission, BER with different tuning speed within a 400-μs time window ranging from 1545 to 1553 nm are measured in Fig. 3(e), and average BERs versus different tuning speeds are given in Fig. 3(f). Even for the fasted tuning speed of 20,000 nm/s, average BER under 1×10^{-3} can still be achieved, showing that PR Rx is robust to ultrafast wavelength tuning which may occur in switching on/off DFB lasers in upstream BM operation.

5. Conclusions

We characterized the performance of the PR Rx reconstructing 40-GBaud QPSK signal under ultrafast wavelength drift up to 20,000 nm/s. Experimental results show that the colorless PR receiving scheme can successfully address the issues of wavelength drift associated with the upstream BM operation in ONU transmitters and is promising to support future high speed PONs.

This work was supported in part by the Science and Technology Commission of Shanghai Municipality (Project No. 20511102400, 20ZR1420900) and 111 project (D20031).

References

1. M. Xu et al., "Adaptive Modulation and Coding Scheme in Coherent PON for Enhanced Capacity and Rural Coverage", Proc. OFC 2021, paper Th5I.4.
2. N. Suzuki et al., "100 Gb/s to 1 Tb/s Based Coherent Passive Optical Network Technology", *Journal of Lightwave Technology*, vol. 36, no. 8, 1485-1491, 2018.
3. K. Kikuchi, "Fundamentals of Coherent Optical Fiber Communications", *Journal of Lightwave Technology*, vol. 34, no. 1, 157-179, 2016.
4. H. Chen et al., "Space-Time Diversity Phase Retrieval Receiver", Proc. OFC 2021, paper Th4D.3.
5. H. Chen et al., "140G/70G Direct Detection PON with >37 dB Power Budget and 40-km Reach Enabled by...", Proc. ECOC 2021, paper Th3C1-PD2.1.
6. A. Zadok et al., "Spectral Shift and Broadening of DFB Lasers Under Direct Modulation", *IEEE Photon. Technol. Lett.*, vol. 10, no. 12, 1709–1711, 1998.
7. P. Tovar et al., "Characterization of the wide band chirp of laser diodes with time-resolved spectroscopy", *Applied Optics*, vol. 58, no. 25, 6737-6741, 2019.
8. H. Chen et al., "Dual Polarization Full-Field Signal Waveform Reconstruction Using ...", *Journal of Lightwave Technology*, vol. 38, no. 9, 2587-2597, 2020.